

44  
BRL-SITE COPY

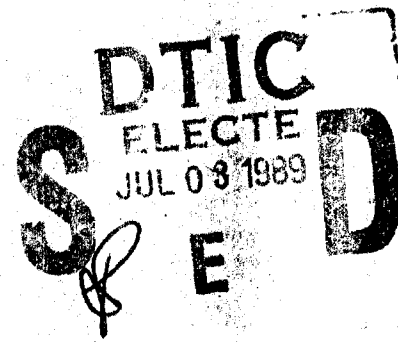
## MEMORANDUM REPORT BRL-MR-3768

AD-A209-510

**BRL**DETERMINATION OF AERODYNAMIC DRAG  
AND EXTERIOR BALLISTIC TRAJECTORY SIMULATION  
FOR THE 155MM, DPICM, M864 BASE-BURN PROJECTILE

ROBERT F. LIESKE

JUNE 1989



APPROVED FOR PUBLIC RELEASE, DISTRIBUTION UNLIMITED.

Best Available Copy

U.S. ARMY LABORATORY COMMAND

BALLISTIC RESEARCH LABORATORY  
ABERDEEN PROVING GROUND, MARYLAND

39 6 30 028

REPORT DOCUMENTATION PAGE

1a. REPORT SECURITY CLASSIFICATION UNCLASSIFIED		1b. RESTRICTIVE MARKINGS	
2a. SECURITY CLASSIFICATION AUTHORITY		3. DISTRIBUTION/AVAILABILITY OF REPORT Approved for public release; distribution is unlimited.	
2b. DECLASSIFICATION/DOWNGRADING SCHEDULE			
4. PERFORMING ORGANIZATION REPORT NUMBER(S) BRL-MR-3768		5. MONITORING ORGANIZATION REPORT NUMBER(S)	
6a. NAME OF PERFORMING ORGANIZATION U.S. Army Ballistic Research Laboratory	6b. OFFICE SYMBOL (If applicable) SLCBR-LF	7a. NAME OF MONITORING ORGANIZATION	
6c. ADDRESS (City, State, and ZIP Code) Aberdeen Proving Ground, MD 21005-5066		7b. ADDRESS (City, State, and ZIP Code)	
8a. NAME OF FUNDING/SPONSORING ORGANIZATION US Army Research, Development and Engineering Center	8b. OFFICE SYMBOL (If applicable)	9. PROCUREMENT INSTRUMENT IDENTIFICATION NUMBER	
8c. ADDRESS (City, State, and ZIP Code) Picatinny Arsenal, NJ 07806-5000		10. SOURCE OF FUNDING NUMBERS	
		PROGRAM ELEMENT NO. F18Y30	PROJECT NO. 77M1AJ
		TASK NO.	WORK UNIT ACCESSION NO.
11. TITLE (Include Security Classification) Determination of Aerodynamic Drag and Exterior Ballistic Trajectory Simulation for The 155mm, DPICM, M864 Base-Burn Projectile			
12. PERSONAL AUTHOR(S) Robert F. Lieske			
13a. TYPE OF REPORT Memorandum Report	13b. TIME COVERED FROM _____ TO _____	14. DATE OF REPORT (Year, Month, Day) 1989 January	15. PAGE COUNT 37
16. SUPPLEMENTARY NOTATION  This report supersedes IMR-891, dated June 1987.			
17. COSATI CODES		18. SUBJECT TERMS (Continue on reverse if necessary and identify by block number) Base-Burn Projectile      Doppler Radar Data Aerodynamic Drag      Flight Performance Trajectory Modeling	
FIELD 19 01	GROUP 01		
01	01		
19. ABSTRACT (Continue on reverse if necessary and identify by block number)  HAWK Doppler radar data collected at Yuma Proving Ground, Arizona for the 155mm, DPICM, M864 base-burn projectile have been reduced for the purpose of determining the aerodynamic drag. The estimated base drag reduction during base-burn motor functioning showed a very good correlation with time of flight and to a lesser degree with local atmospheric air pressure. No correlation was evident with flight Mach number, provided an effective base drag coefficient is assumed which is just a function of Mach number. This result suggests a simple addition to the Modified Point Mass Trajectory Model for the exterior ballistic simulation of the M864 base-burn projectile. <i>Keywords: Projectile trajectories, DPICM (Dual-purpose Improved Conventional Munitions), Propellant burning, Ballistic trajectory modeling.</i> (ed.)			
20. DISTRIBUTION/AVAILABILITY OF ABSTRACT <input type="checkbox"/> UNCLASSIFIED/UNLIMITED <input checked="" type="checkbox"/> SAME AS RPT. <input type="checkbox"/> DTIC USERS		21. ABSTRACT SECURITY CLASSIFICATION UNCLASSIFIED	
22a. NAME OF RESPONSIBLE INDIVIDUAL ROBERT F. LIESKE		22b. TELEPHONE (Include Area Code) 301-278-3577	22c. OFFICE SYMBOL SLCBR-LF-T

### Acknowledgement

The author would like to express his appreciation to Mr. Joseph A. Hurff for preparing the computer programs required to calculate the aerodynamic drag results and to Mrs. Margaret S. Wilson and Messrs. Joseph M. Wall and Joseph W. Kochenderfer for assembling and reducing the 155mm, DPICM, M864 base-burn projectile range data. The author also wishes to acknowledge the numerous helpful comments and suggestions received from Dr. James E. Danberg.

<b>Accession For</b>	
NTIS GRA&I	<input type="checkbox"/>
DTIC TAB	<input type="checkbox"/>
Unannounced	<input type="checkbox"/>
<b>Justification</b>	
<b>By</b>	
<b>Distribution/</b>	
<b>Availability Codes</b>	
Dist	Avail and/or Special
A-1	



## Table of Contents

	<u>Page</u>
List of Figures . . . . .	vii
I. Introduction . . . . .	1
II. Reduction of HAWK Doppler Radar Velocimeter Flight Data . . . . .	1
III. Determination of Aerodynamic Drag Coefficient . . . . .	2
IV. Determination of Base Drag Reduction Factor . . . . .	3
V. Results . . . . .	3
VI. Analysis of Aerodynamic Drag Results . . . . .	4
VII. Exterior Ballistic Trajectory Simulation Model . . . . .	5
VIII. Conclusions . . . . .	7
References . . . . .	27
List of Symbols . . . . .	29
Distribution List . . . . .	31

## List of Figures

<u>Figure</u>		<u>Page</u>
1	Physical characteristics of the 155mm, DPICM, M864 base-burn projectile.	8
2	Aerodynamic drag coefficient versus Mach number for round number 4315, with inert base-burn motor, fired with propelling charge M4A2, 7W, at a quadrant elevation of 748 mils. . . . .	9
3	Aerodynamic drag coefficient versus Mach number for round number 4376, with inert base-burn motor, fired with propelling charge M119A2, 7R, at a quadrant elevation of 748 mils. . . . .	10
4	Aerodynamic drag coefficient versus Mach number for round number 4341, with inert base-burn motor, fired with propelling charge M203E2, 8R, at a quadrant elevation of 748 mils. . . . .	11
5	Base drag reduction factor versus time of flight for round number 5089 fired with propelling charge M4A2, 7W, at a quadrant elevation of 500 mils. . . .	12
6	Base drag reduction factor versus time of flight for round number 1034 fired with propelling charge M4A2, 7W, at a quadrant elevation of 750 mils. . . .	13
7	Base drag reduction factor versus time of flight for round number 1013 fired with propelling charge M4A2, 7W, at a quadrant elevation of 1150 mils. . . .	14
8	Base drag reduction factor versus time of flight for round number 1044 fired with propelling charge M119A2, 7R, at a quadrant elevation of 500 mils. . . .	15
9	Base drag reduction factor versus time of flight for round number 1050 fired with propelling charge M119A2, 7R, at a quadrant elevation of 750 mils. . . .	16
10	Base drag reduction factor versus time of flight for round number 4202 fired with propelling charge M119A2, 7R, at a quadrant elevation of 1150 mils. . . .	17
11	Base drag reduction factor versus time of flight for round number 4216 fired with propelling charge M203E2, 8R, at a quadrant elevation of 499 mils. . . .	18
12	Base drag reduction factor versus time of flight for round number 4329 fired with propelling charge M203E2, 8R, at a quadrant elevation of 748 mils. . . .	19
13	Base drag reduction factor versus time of flight for round number 4219 fired with propelling charge M203E2, 8R, at a quadrant elevation of 1147 mils. . . .	20
14	Aerodynamic drag force coefficients for the 155mm, DPICM, M864 base-burn projectile. . . . .	21
15	Factor $f_1$ versus Mach number for the 155mm, DPICM, M864 projectile. . . .	22
16	Factor $f_2$ versus time of flight for the 155mm, DPICM, M864 projectile. . . .	23

## List of Figures (Continued)

<u>Figure</u>		<u>Page</u>
17	Residuals of the stepwise multiple regression analysis versus time of flight. .	24
18	Residuals of the stepwise multiple regression analysis versus Mach number.	25
19	Residuals of the stepwise multiple regression analysis versus local air pressure.	26

## I. Introduction

The Modified Point Mass Trajectory Model <sup>1,2</sup> is the primary method of trajectory simulation used in the preparation of Firing Tables. This model requires three types of input data: projectile mass properties, aerodynamic coefficients and the performance parameters determined from range testing. This report discusses an initial attempt to determine, for trajectory modeling, the aerodynamic drag of the 155mm, DPICM, M864 base-burn projectile (Figure 1) from the HAWK Doppler radar data.<sup>3,4</sup> A detailed treatise of base-burn projectile ballistic modeling technology is reported by Niles-Erik Gunners, Kurt Andersson and Rune Hellgren in Reference 5, Chapter 16, "Base-Bleed Systems for Gun Projectiles".

## II. Reduction of HAWK Doppler Radar Velocimeter Flight Data

The frame of reference for all vectors is a ground-fixed, orthonormal, right-handed Cartesian coordinate system with unit vectors ( $\vec{1}$ ,  $\vec{2}$  and  $\vec{3}$ ). The  $\vec{1}$  axis is the intersection of the vertical plane of fire and the horizontal plane and pointing in the direction of fire. The  $\vec{2}$  axis is parallel to the gravity vector,  $\vec{g}$ , and opposite in direction. The  $\vec{3}$  axis completes the right-handed coordinate system.

The slant range rate of change as measured by HAWK Doppler radar is recorded on a digital tape. The first step is to smooth the data and determine the time derivative. Least squares fits (second-degree polynomials) to the data are determined for 0.56 second intervals (fifteen point smoothing) along the trajectory. The slant range rate of change ( $\vec{r}$ ) and time derivative of the slant range rate of change ( $\vec{r}'$ ) are obtained from the quadratic fit at the midpoint of the fifteen point interval.

An estimated trajectory is generated separately using the projectile mass properties, launch data, atmospheric conditions, estimated aerodynamic coefficients and estimated base drag reduction factor during base-burn motor burning as a function of time. The trajectory is adjusted, using factors on base drag reduction during motor functioning and lift, to match the observed impact data. A trajectory velocity ( $\vec{u}_t$ ) is calculated using the HAWK radar smoothed slant range rate of change ( $\vec{r}$ ) and the estimated trajectory slant range rate of change ( $\vec{r}_t$ ) and velocity ( $\vec{u}_t$ ) as follows:

$$\vec{u}_r = (\vec{r} / \vec{r}_t) \vec{u}_t \quad (1)$$

where:

$$\vec{r}_t = u_t \cos(r_t, u_t) = (\vec{r}_t \cdot \vec{u}_t) / r_t$$

Note: Subscript  $t$  refers to quantities determined from the estimated trajectory and those with subscript  $r$  are obtained using both the HAWK radar data and the estimated trajectory.

A trajectory acceleration ( $\dot{\vec{u}}_r$ ) was calculated using the time derivative of the HAWK radar slant range rate of change ( $\ddot{r}$ ) and the estimated trajectory, time derivative of the slant range rate of change ( $\ddot{r}_t$ ) and acceleration ( $\vec{u}_t$ ), using the following two formulations:

$$\dot{\vec{u}}_r = (\dot{r} / \dot{r}_t) \dot{\vec{u}}_t + [(\dot{r}_t \ddot{r} - \dot{r} \ddot{r}_t) / \dot{r}_t^2] \vec{u}_t \quad (2)$$

and

$$\dot{\vec{u}}_r = (\ddot{r} / \dot{r}_t) \dot{\vec{u}}_t \quad (3)$$

where:

$$\ddot{r}_t = \{ r_t [(\dot{\vec{r}}_t \cdot \vec{u}_t) + (\vec{r}_t \cdot \dot{\vec{u}}_t)] - (\vec{r}_t \cdot \vec{u}_t) \dot{r}_t \} / r_t^2$$

and

$$\dot{\vec{r}}_t = \vec{u}_t$$

The mean of the results were similar for both of the  $\dot{\vec{u}}_r$  representations, however, the variation (spread) of the results were significantly improved using equation 3 and it was used for determining the results presented.

### III. Determination of Aerodynamic Drag Coefficient

The mass of the projectile, atmospheric conditions, estimated trajectory data and the Doppler slant range rate of change and time derivative of the slant range rate of change provide the necessary inputs to determine the aerodynamic drag. The following inverse solution of the point-mass equations of motion is then used to compute the aerodynamic drag ( $C_{D,r}$ ).

$$C_{D,r} = -[(\vec{u}_r - \vec{w}) \cdot (\dot{\vec{u}}_r - \vec{g} - \vec{\Lambda})] 8 m / (\pi \rho d^2 v^3) \quad (4)$$

#### IV. Determination of Base Drag Reduction Factor

The base-burn motor is intended to increase the range of the projectile by reducing the base drag. An initial estimate of the aerodynamic zero yaw drag force coefficient ( $C_{D_0}$ ) and the base drag component ( $C_{D_B}$ ) was determined for the M864 base-burn projectile, with an inert base-burn motor, using the semi-empirical drag estimation model known as McDrag.<sup>6</sup> A base drag reduction factor ( $f_{BD}$ ) was then defined to quantify the amount of base drag reduction as follows:

$$f_{BD} = (C_{D_0} - C_{D_B}) / C_{D_B} \quad (5)$$

A base drag reduction factor of unity indicates that all the estimated base drag is eliminated, whereas a value of zero means none of the estimated base drag is eliminated. A  $f_{BD}$  greater than one indicates that thrusting is present, since more than just the base drag has been eliminated.

#### V. Results

The aerodynamic drag results, obtained from the procedure described above, are presented for a sampling of the M864 projectiles, including three M864 projectiles with inert base-burn motors. These projectiles were fired at Yuma Proving Ground, AZ during May 1987. The base-burn motors were designed to burn out at approximately 30 seconds. The aerodynamic drag coefficients for the projectiles with inert motors are presented as a function of Mach number and for the projectiles with live motors base drag reduction factors are presented as a function of time of flight.

The sampling includes projectiles with inert and live base-burn motors fired with propelling charges: M4A2, charge 7W; M119A2, charge 7R; and M203E2, charge 8R. The sampling contains an inert base-burn motor fired at a quadrant elevation of 748 mils and live base-burn motors fired at three quadrant elevations (approximately 500, 750 and 1150 mils) with each of the propelling charges.

Figures 2 through 4 present the aerodynamic drag coefficients versus Mach number for projectiles with inert base-burn motors fired with each of the propelling charges at a quadrant elevation of 748 mils. Figures 5 through 13 present the base drag reduction factors versus time of flight for projectiles with live base-burn motors fired with each of the propelling charges at quadrant elevations of approximately 500, 750 and 1150 mils.

Figures 2, 3 and 4 show excellent agreement of the aerodynamic drag coefficients for the inert base-burn motor projectiles fired with the three propelling charges. Figures 5 through 13 show a good correlation of the base drag reduction factor with time of flight for the live base-burn motor projectiles. The base drag is consistently reduced by approximately 50 percent and the results show an increase in this percentage for the higher quadrant elevations indicating a possible correlation with local atmospheric pres-

sure. There is some irregularity in the base drag reduction factor for the transonic velocities (Mach numbers: .95 to 1.05). This is identified where evident on some of the figures. The irregularity is probably due to the error in the transonic aerodynamic inputs and/or the Mach number determined from the HAWK radar data. The base drag reduction factors also indicate a delay in base drag reduction at the beginning of approximately one second and a base-burn motor burnout time of approximately 33 seconds.

The large variation in the base drag reduction factor for the high quadrant elevation rounds is probably due to a combination of the following: the magnitude of the total drag coefficient, the data reduction methodology including the estimated trajectory, the estimated aerodynamic coefficients and the HAWK Doppler radar capability.

## VI. Analysis of Aerodynamic Drag Results

An aerodynamic drag coefficient  $C_{D_0}$  was determined for the M864 projectile based on the inert base-burn motor projectile results. In addition, an estimated inert, base drag component  $C_{D_{B_i}}$  was determined for the M864 projectile with an inert base-burn motor by subtracting the McDrag estimates of head, skin friction, band and boat tail drag from the determined  $C_{D_0}$  for the inert M864 projectile. Figure 14 presents the determined  $C_{D_0}$  and  $C_{D_{B_i}}$  functions of Mach number.

The base drag reduction factors for times of flight between three and 33 seconds were analyzed using a stepwise multiple regression technique.<sup>7</sup> The base drag reduction factors were fit as a function of time of flight and the difference in a reference (standard) air pressure ( $P_r$ ), 1013.25 mb, and the local air pressure ( $P$ ) divided by  $P_r$  to account for the apparent variation with quadrant elevation. A review of the residuals as a function of Mach number suggested an additional function of Mach number,  $f_1$ , which forms a modified base drag coefficient, ( $C_{D_{B_i}} f_1$ ), for the M864 base-burn projectile. Figure 14 presents the modified base drag coefficient, ( $C_{D_{B_i}} f_1$ ), while Figure 15 presents the  $f_1$  factor as a function of Mach number. The value of ( $C_{D_{B_i}} f_1$ ) is 25 percent higher for Mach numbers less than 0.9 and 11 percent lower at Mach number 2.0 than the theoretically determined  $C_{D_{B_i}}$ . A theoretical discussion of drag reduction for base-burn projectiles is presented in Reference 5, Chapter 16.

The stepwise multiple regression fitting function including  $f_1$  is as follows:

$$[(C_{D_0} - C_{D_r}) / (C_{D_{B_i}} f_1)] = f_2 + f_4 (P_r - P) / P_r \quad (6)$$

Where:

- Factor  $f_2$  is a function of time of flight.
- Factor  $f_4$  is a constant.

Note: A factor  $f_3$  multiplying  $f_2$  is added in the final formulation.

The factor,  $f_2$ , as a function of time of flight, determined by the stepwise multiple regression process for the nine M864 base-burn test projectiles (Figures 5 through 13), is presented in Figure 16 and the constant,  $f_4$ , determined simultaneously, was 0.30. The residuals of the stepwise multiple regression fitting process are presented in Figures 17, 18 and 19 versus time of flight, Mach number and local air pressure respectively. The root mean square error of residuals is 0.12 and the residuals show that the fitting process has removed the symmetric biases due to time of flight, Mach number and local air pressure.

Summarizing:

- An aerodynamic drag coefficient ( $C_{D_0}$ ) was determined for the M864 projectile based on the inert base-burn motor projectile results.
- A base drag component ( $C_{D_{B_i}}$ ) was theoretically determined for the M864 projectile with an inert base-burn motor based on  $C_{D_0}$  minus the fore body drag estimated by McDrag.
- A factor,  $f_1$ , multiplied by the inert projectile base drag component ( $C_{D_{B_i}}$ ) is used to represent an effective inert base drag coefficient for the M864 base-burn projectile as a function of Mach number.
- A factor,  $f_2$ , is used to represent the effect of time on drag reduction during the burning phase of the M864 base-burn projectile.
- A change in drag reduction with local air pressure was assumed to account for the observed variation of the M864 base-burn projectile base drag with quadrant elevation. This apparent effect with local air pressure was further assumed to take the form  $f_4 (P_r - P) / P_r$ , where the factor,  $f_4$ , is a constant.

## VII. Exterior Ballistic Trajectory Simulation Model

The reduction in base drag during base-burn motor functioning is shown to be a function of time of flight and to a lesser degree a function of local air pressure. A constant,  $f_3$ , multiplied by  $f_2$  is added to create a simulation methodology containing flexibility for matching experimental radar and impact or air burst data. The constants,  $f_3$  and  $f_4$ , can then be used effectively as parameters for matching the measured impact or air burst range firing data.

The combined base drag reduction term,  $-(C_{D_{B_i}} f_1) [f_2 f_3 + f_4 (P_r - P) / P_r]$ , is then added to the projectile's inert total drag force coefficient term,  $C_{D_0} + C_{D_{a2}} (Q\alpha_e)^2$ , of the Modified Point Mass Trajectory Model for Rocket Assisted Projectiles.

The total drag computed by the Modified Point Mass Trajectory Model for Rocket Assisted Projectiles is then as follows:

$$\tilde{D} = -\frac{\pi \rho d^2 f_0}{8 m} \{ C_{D_0} - (C_{D_B} f_1) [f_2 f_3 + f_4 (P_r - P) / P_r] + C_{D_a} (Q \alpha_e)^2 \} v \tilde{v} \quad (7)$$

Where:

- The factor,  $f_0$ , can be used as a function of quadrant elevation, instead of the ballistic coefficient, for matching experimental impact or air burst range firing data for projectiles without base-burn motors. A value of 1.0 was used for  $f_0$  because this parameter was not used for matching the experimental firing data of the M864 base-burn projectile.

Note: The ballistic coefficient,  $m_r / (f_0 d^2)$ , as a function of quadrant elevation is currently in use as the parameter for matching experimental impact or air burst range firing data. The use of  $f_0$ , previously identified as  $i$ , has the advantage of being a nondimensional factor.

- The term,  $(C_{D_B} f_1) (f_2 f_3)$ , is used to represent the drag reduction as a function of Mach number and time of flight and for matching experimental impact or air burst range firing data of individual or groups of projectiles.
  - The factor,  $f_1$ , as illustrated in Figure 15, is used to represent the change in drag reduction as a function of Mach number.  $f_1$  was determined from the analysis of the HAWK radar data.
  - The factor,  $f_2$ , as illustrated in Figure 16, is used to represent the change in drag reduction as a function of time of flight.  $f_2$  was also determined from the analysis of the HAWK radar data.
  - The factor,  $f_3$  can be used as a parameter for matching experimental impact or air burst range firing data.
- The term,  $(C_{D_B} f_1) [f_4 (P_r - P) / P_r]$ , is used to represent the drag reduction due to an apparent effect of the local air pressure.
  - The factor,  $f_4$ , is a constant during base-burn motor functioning and is zero thereafter.  $f_4$  was determined to be 0.30 based on the analysis of the HAWK radar data.
- The factor,  $Q$ , is a constant used to compensate in part for the approximations in the Modified Point Mass Trajectory Model. A value 1.2, normally used for artillery projectiles, was used for this parameter.

In the above model the nondimensional factor,  $f_0$ , replaces the ballistic coefficient as the parameter used for matching experimental impact or air burst range firing data of projectiles without base-burn. In that role,  $f_0$  would normally be a function of quadrant elevation. The factors,  $f_1$  through  $f_4$ , should be effective parameters for representing the HAWK radar results and matching the experimental impact or air burst range firing data of the 155mm, M864 base-burn projectile.

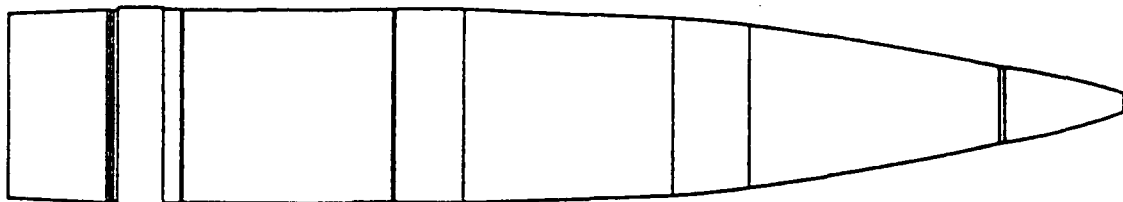
## VIII. Conclusions

The aerodynamic drag coefficients determined for the M864 projectiles with inert base-burn motors show excellent agreement for the flight Mach numbers of projectiles fired with propelling charges: M4A2, charge 7W; M119A2, charge 7R; and M203E2, charge 8R.

The reduction in base drag during base-burn motor functioning correlated very well with time of flight and to a lesser degree with local air pressure. These results support the simplistic addition of a base drag reduction term to the acceleration due to drag equation of the Modified Point Mass Trajectory Model for Rocket-Assisted Projectiles for simulating the ballistic trajectory of the 155mm, M864 base-burn projectile.

## 155mm, DPICM, M864 Base-Burn Projectile

### Sketch



### Dimensions

Length of Projectile	calibers	5.79
Nose Length	calibers	3.42
Cylinder Length	calibers	1.86
Boattail Length	calibers	.50
Boattail Angle	degrees	3.00

### Mass Properties

Mass	kgs (lbs)	46.95 103.5
Mass of Fuel	kgs (lbs)	1.21 2.67
Center of Gravity	cm from nose (in from nose)	58.8 23.16

### Moments of Inertia

Axial	$\text{kg}\cdot\text{m}^2$ ( $\text{lb}\cdot\text{ft}^2$ )	.158 3.75
Transverse	$\text{kg}\cdot\text{m}^2$ ( $\text{lb}\cdot\text{ft}^2$ )	1.657 39.32

**Figure 1. Physical characteristics of the 155mm, DPICM, M864 base-burn projectile.**

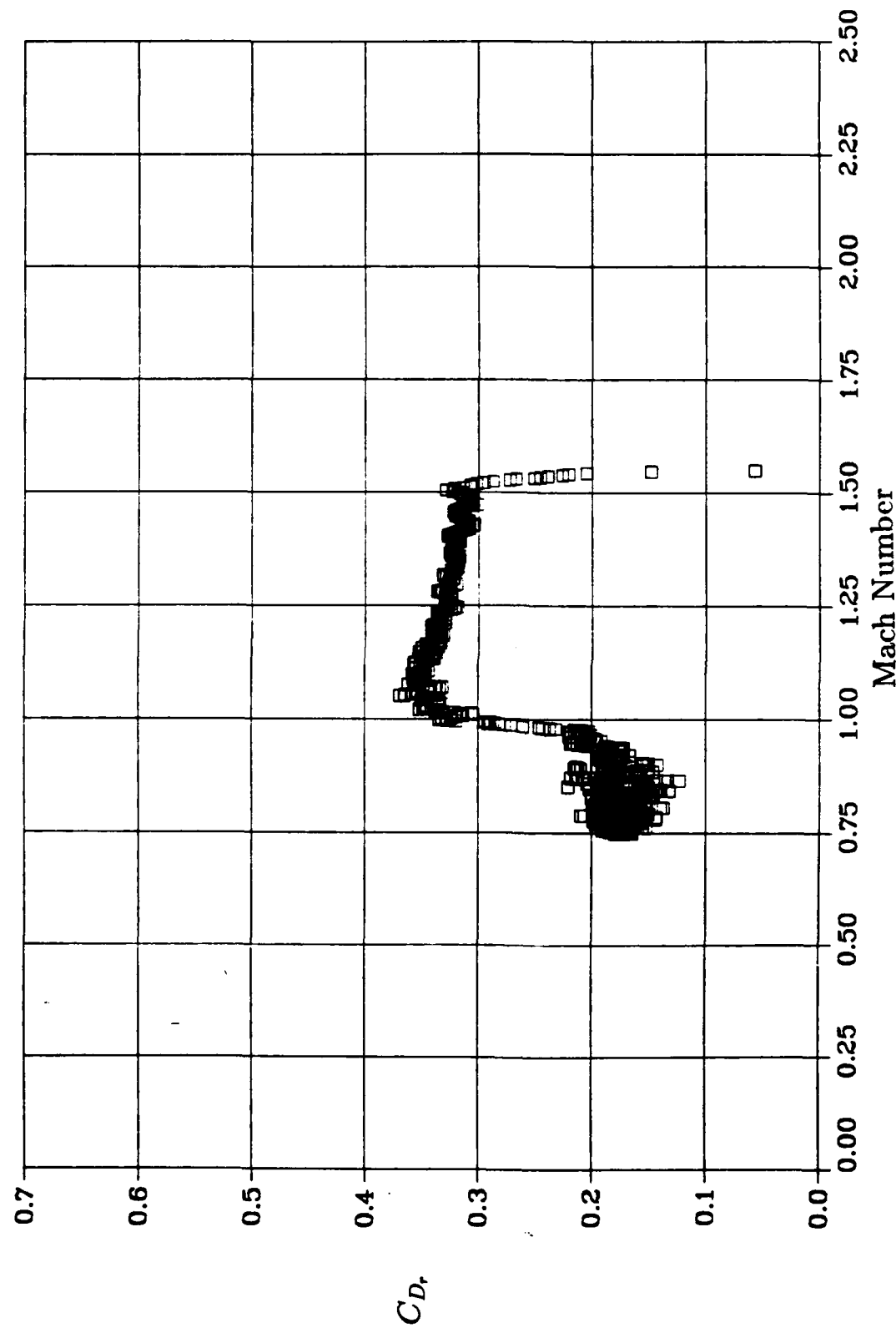


**Figure 2.** Aerodynamic drag coefficient versus Mach number for round number 4315, with inert base-burn motor, fired with propelling charge M4A2, 7W, at a quadrant elevation of 748 mils.

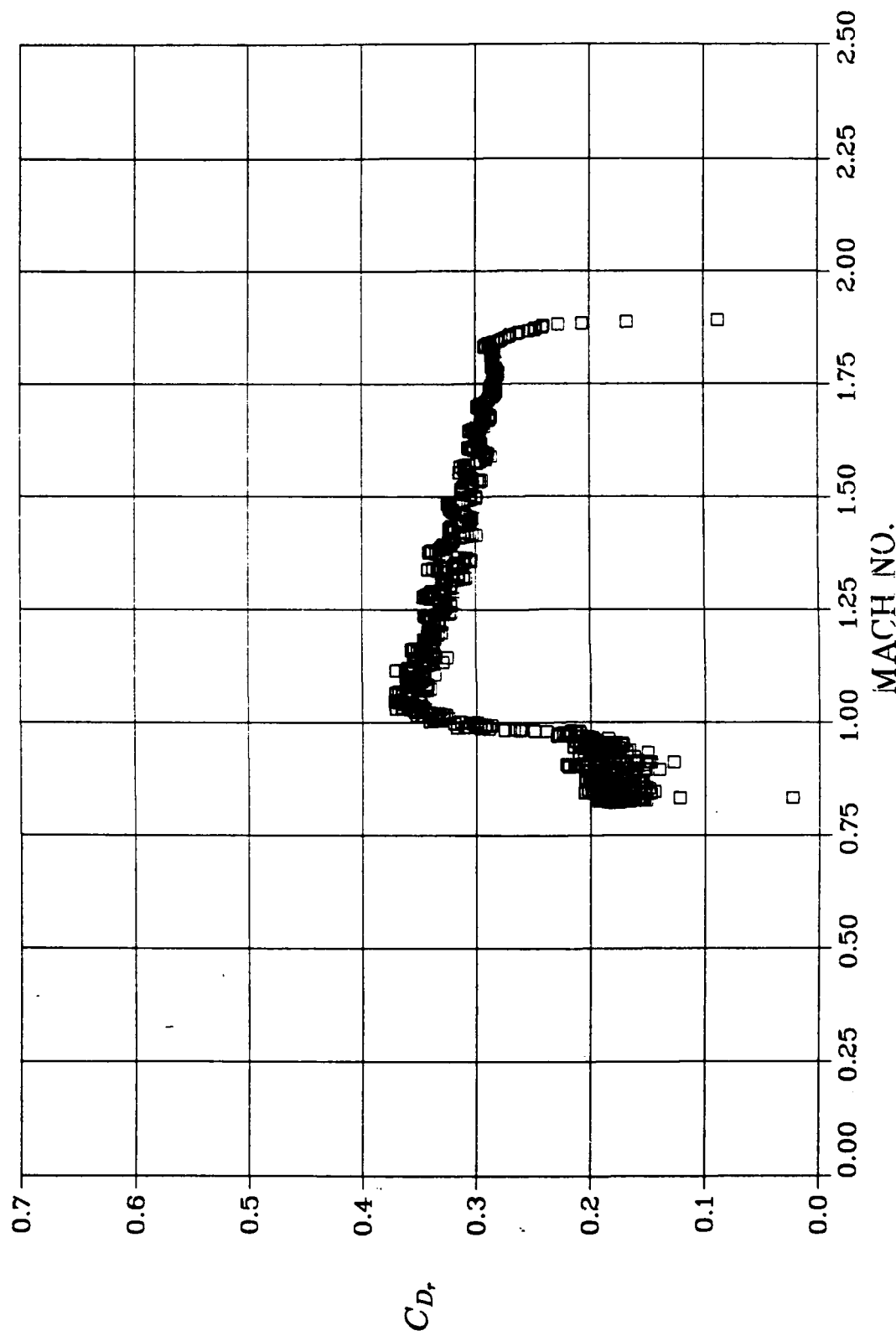
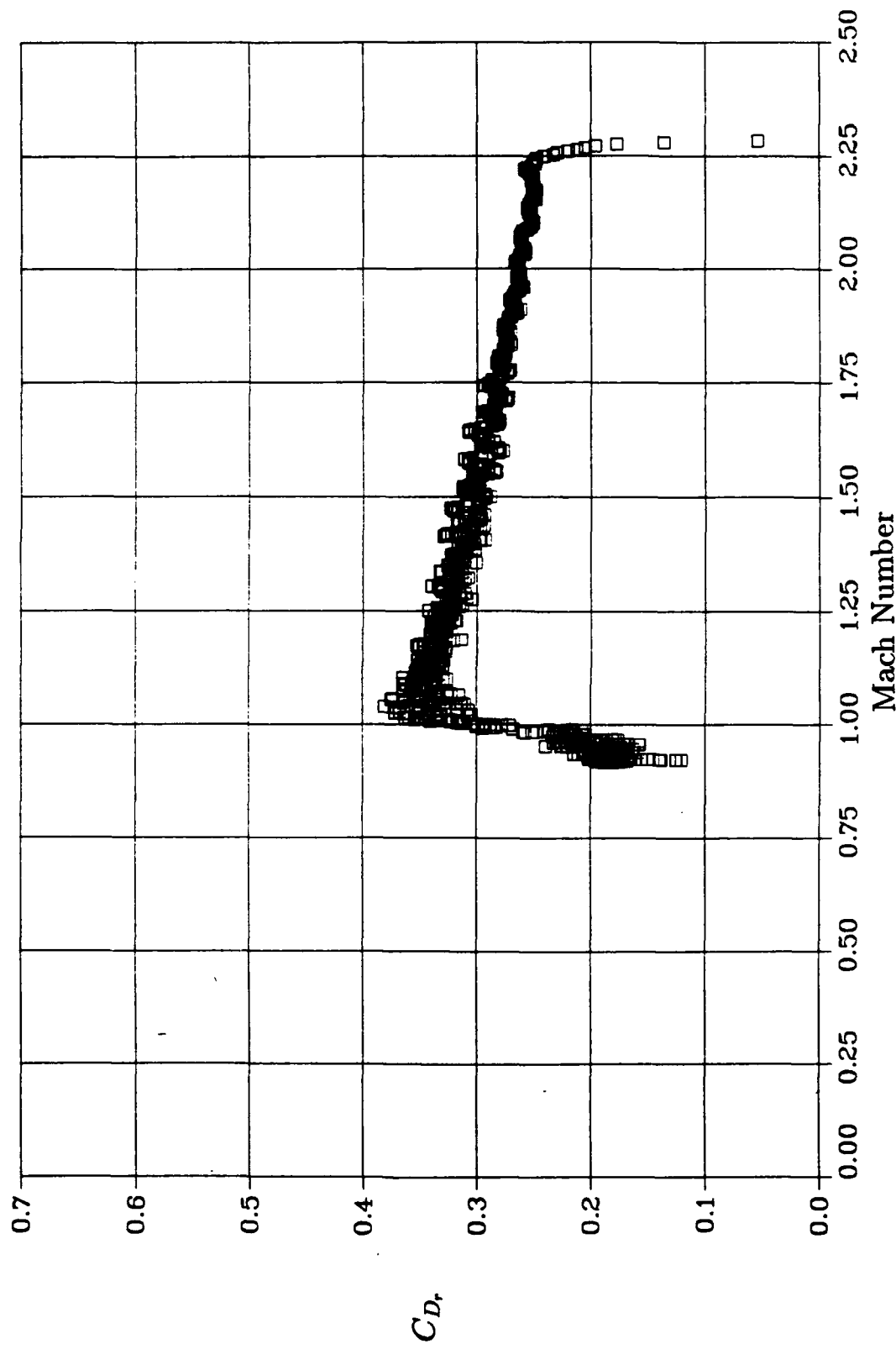
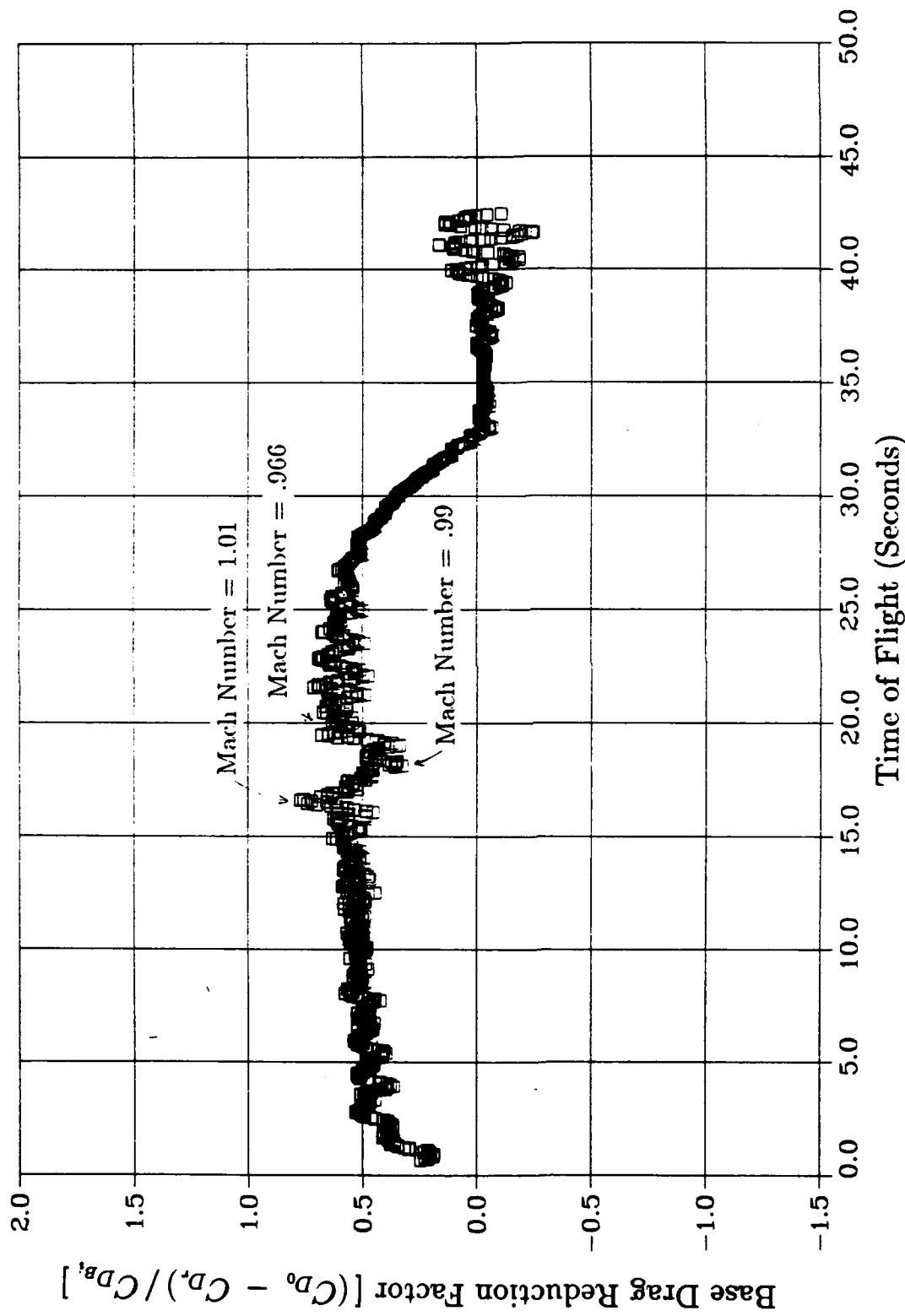


Figure 3. Aerodynamic drag coefficient versus Mach number for round number 4376, with inert base-burn motor, fired with propelling charge M119A2, 7R, at a quadrant elevation of 748 mils.



**Figure 4.** Aerodynamic drag coefficient versus Mach number for round number 4341, with inert base-burn motor, fired with propelling charge M203E2, 8R, at a quadrant elevation of 748 mils.



**Figure 5.** Base drag reduction factor versus time of flight for round number 5089 fired with propelling charge M4A2, 7W, at a quadrant elevation of 500 mils.

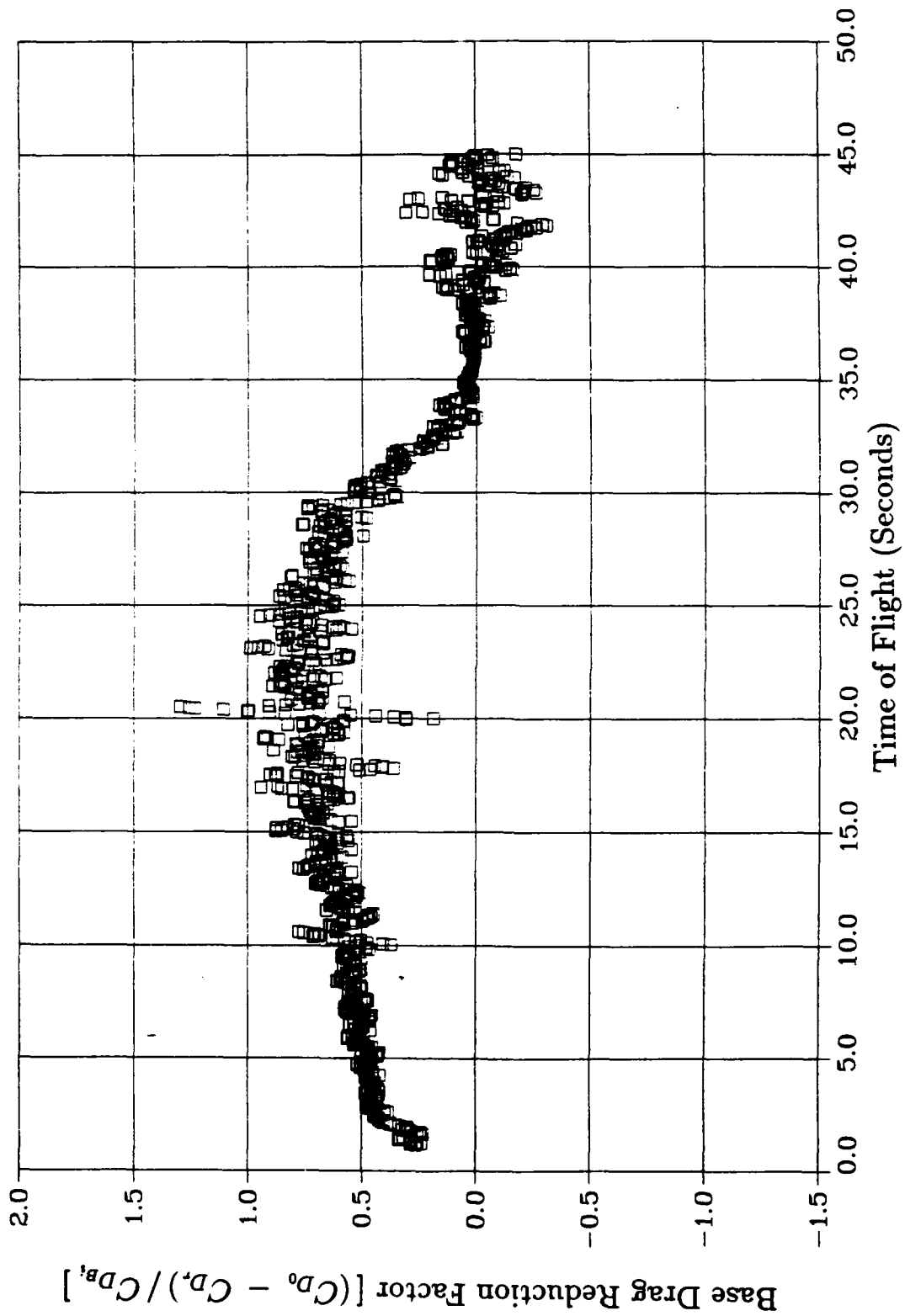


**Figure 6.** Base drag reduction factor versus time of flight for round number 1034 fired with propelling charge M4A2, 7W, at a quadrant elevation of 750 mils.

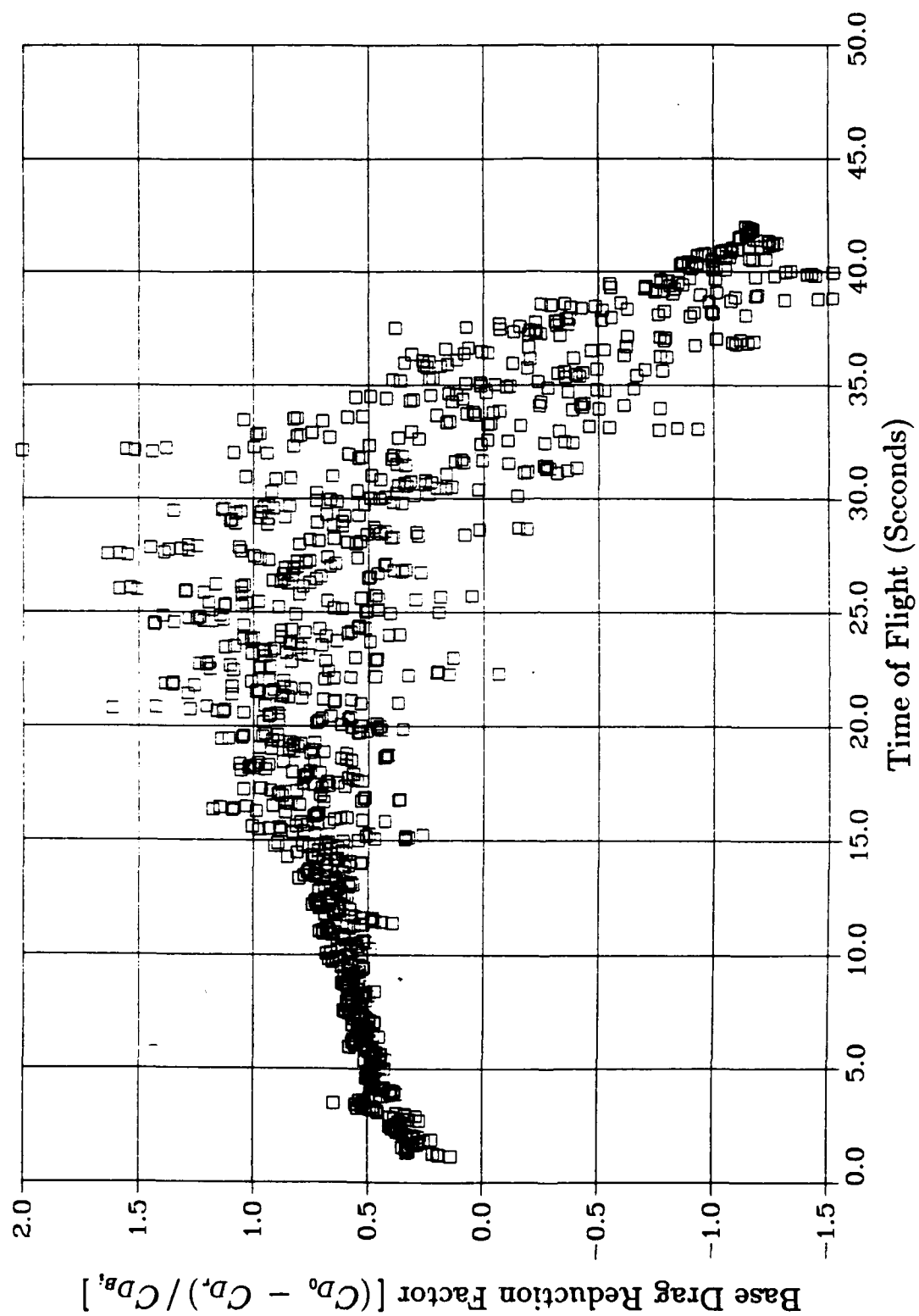


**Figure 7.** Base drag reduction factor versus time of flight for round number 1013 fired with propelling charge M4A2, 7W, at a quadrant elevation of 1150 mils.

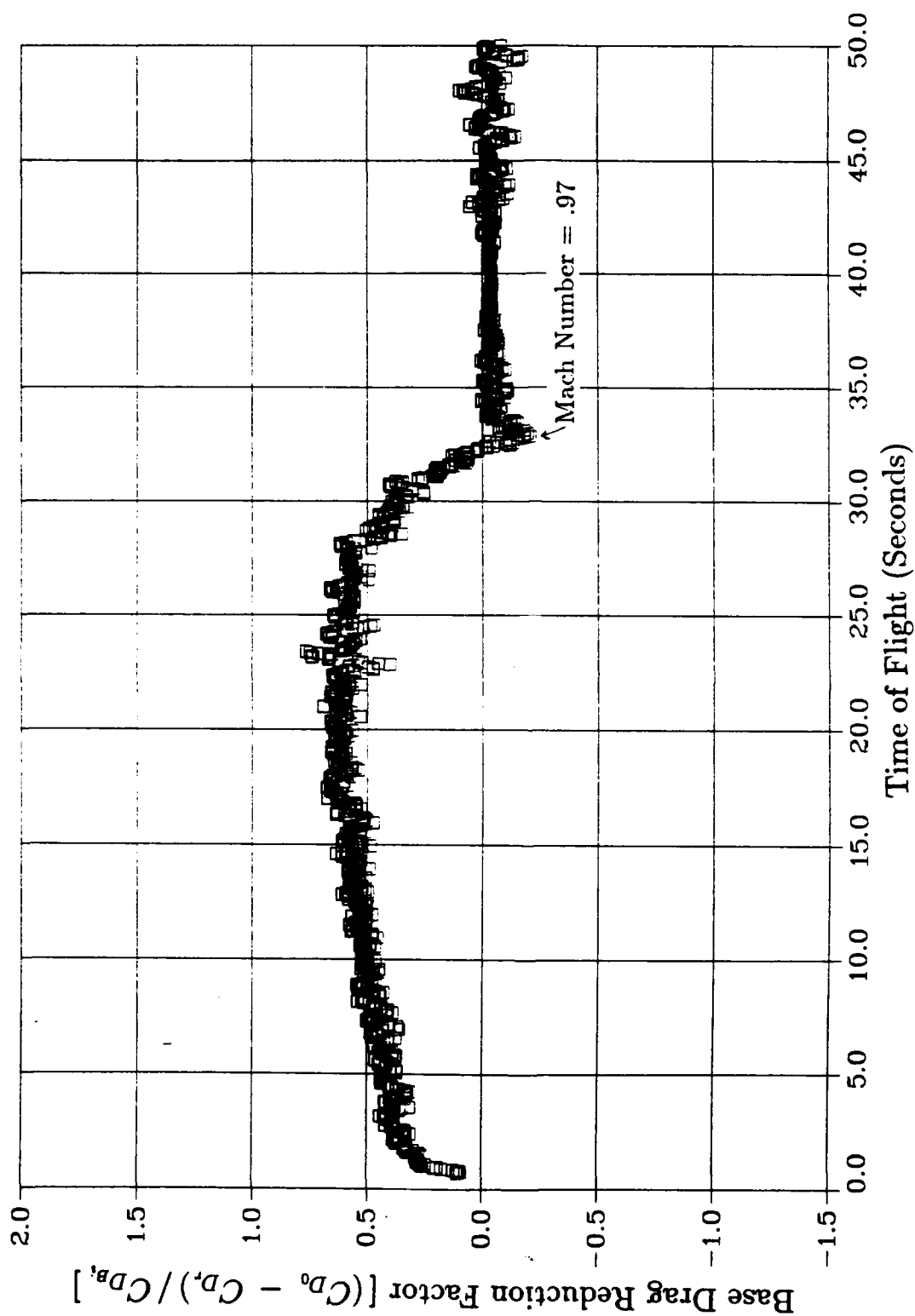


**Figure 8.** Base drag reduction factor versus time of flight for round number 1044 fired with propelling charge M119A2, 7R, at a quadrant elevation of 500 mils.

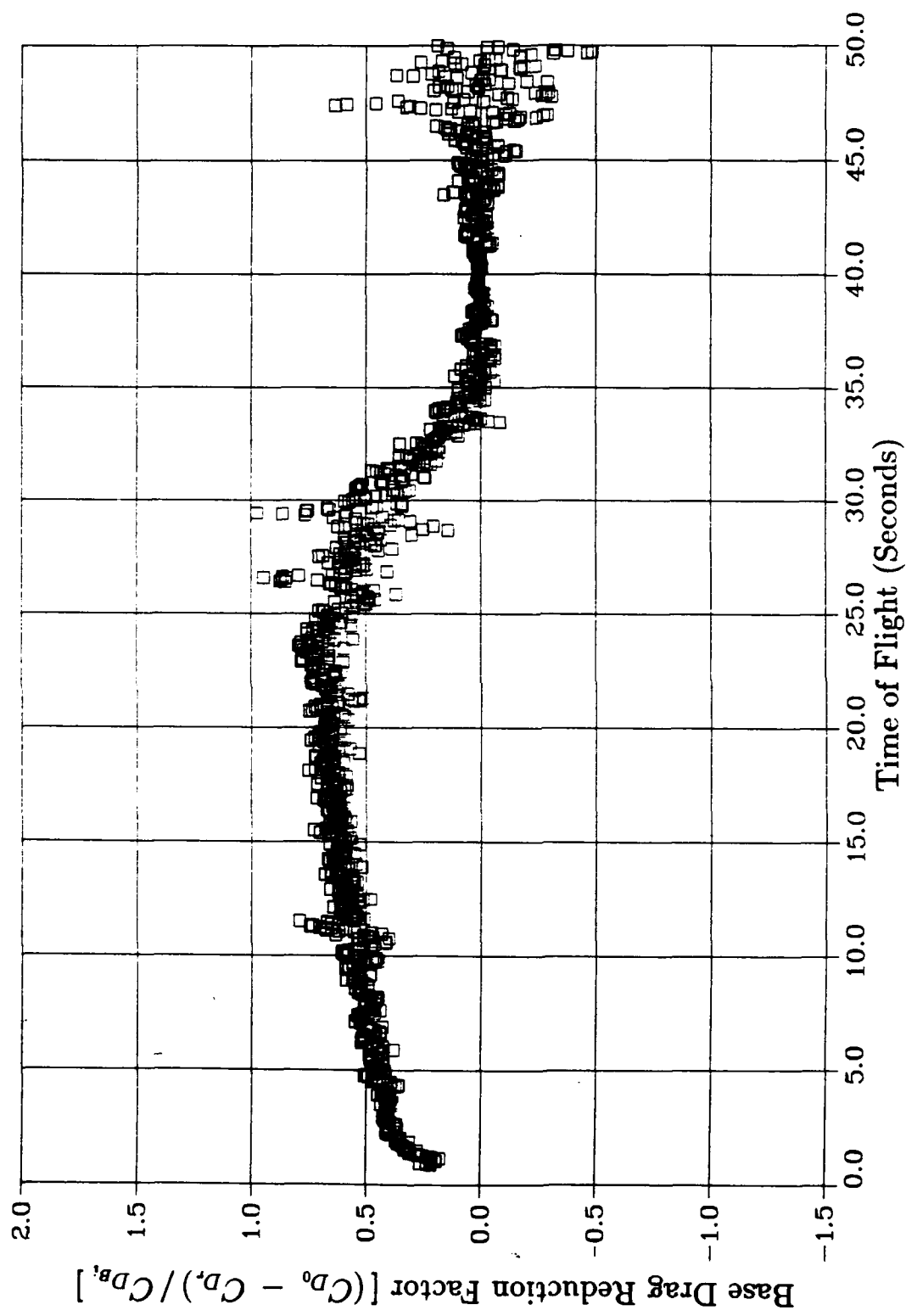


**Figure 9.** Base drag reduction factor versus time of flight for round number 1050 fired with propelling charge M119A2, 7R, at a quadrant elevation of 750 mils.

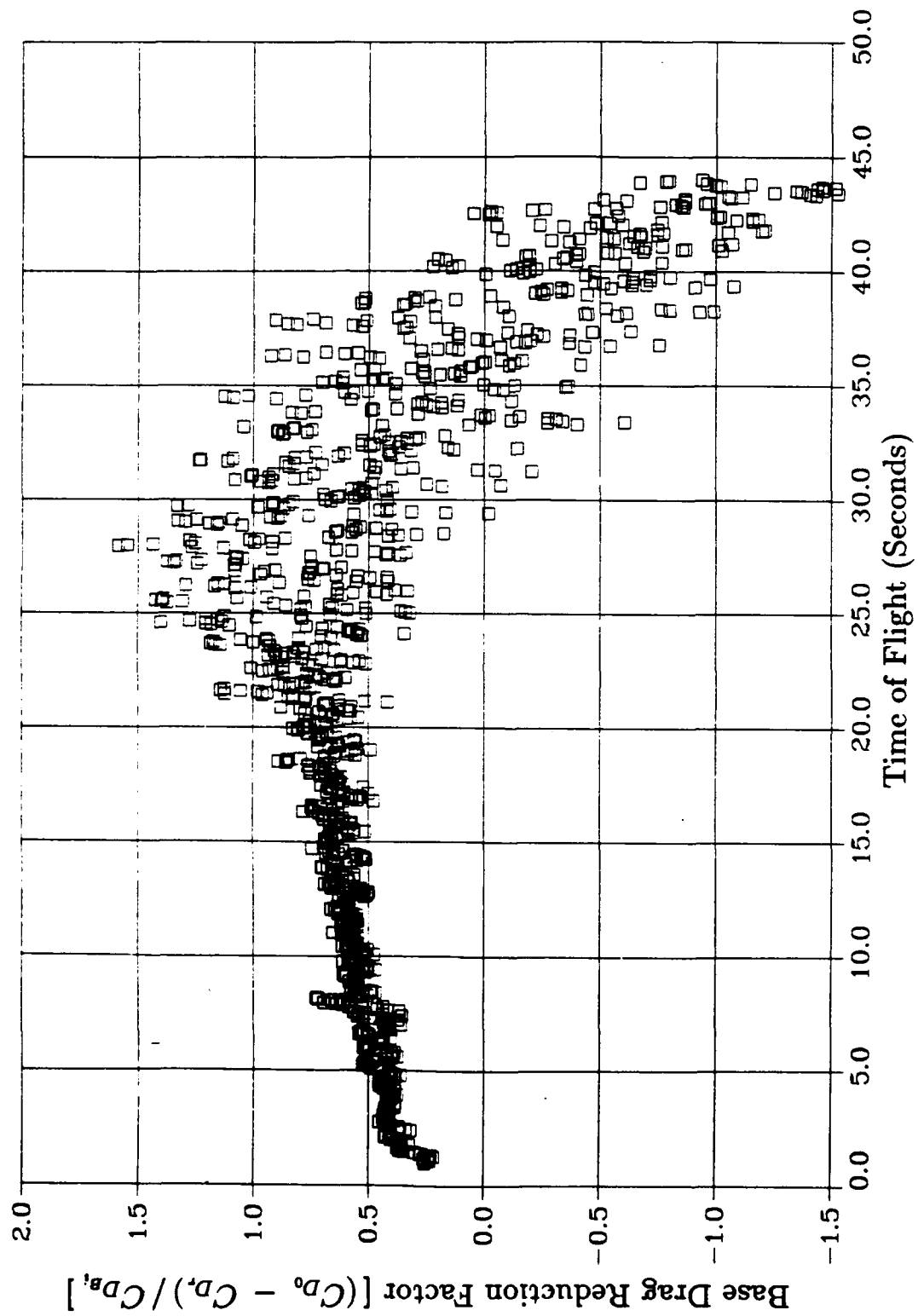


**Figure 10.** Base drag reduction factor versus time of flight for round number 4202 fired with propelling charge M119A2, 7R, at a quadrant elevation of 1150 mils.

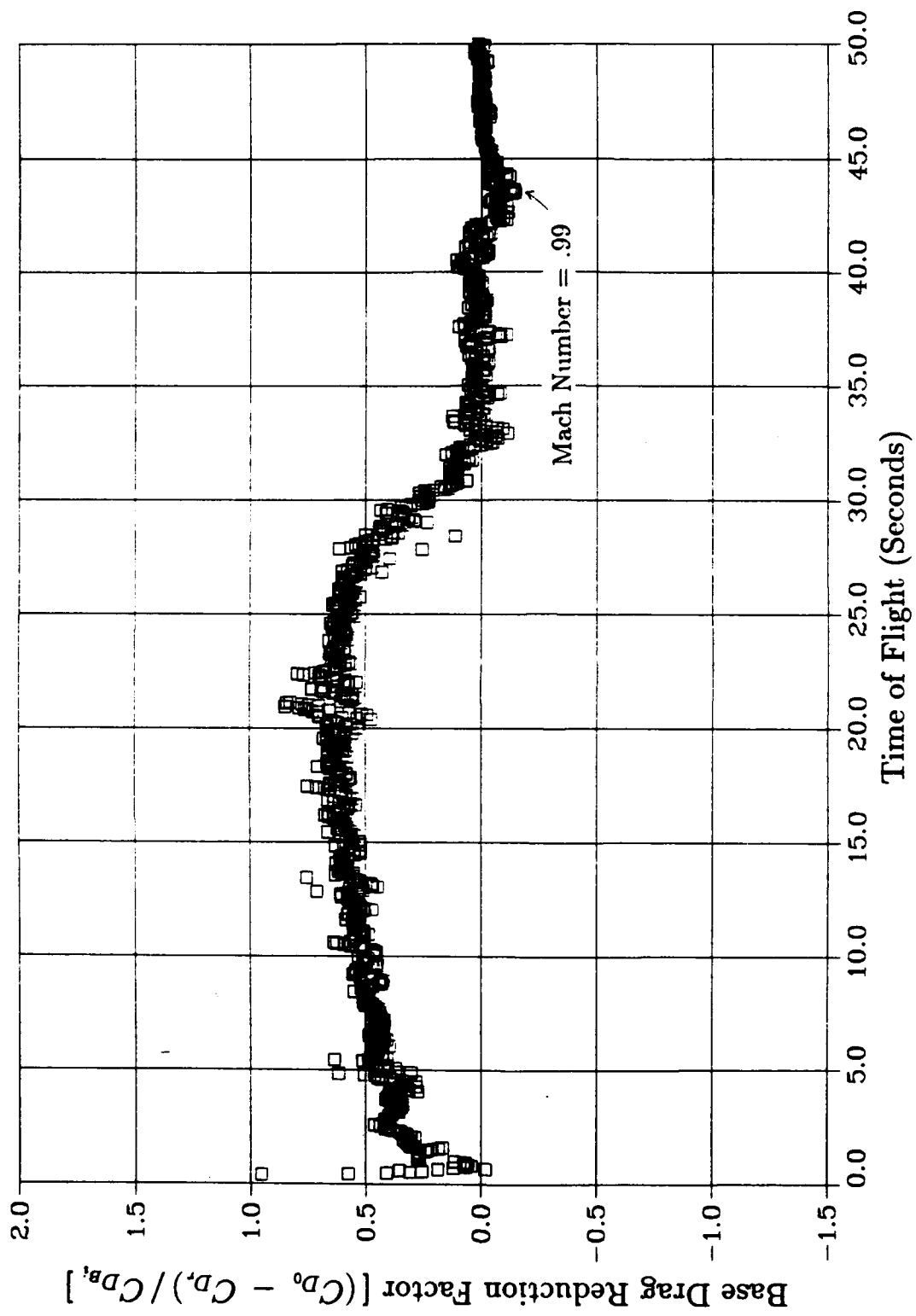


**Figure 11.** Base drag reduction factor versus time of flight for round number 4216 fired with propelling charge M203E2, 8R, at a quadrant elevation of 499 mils.

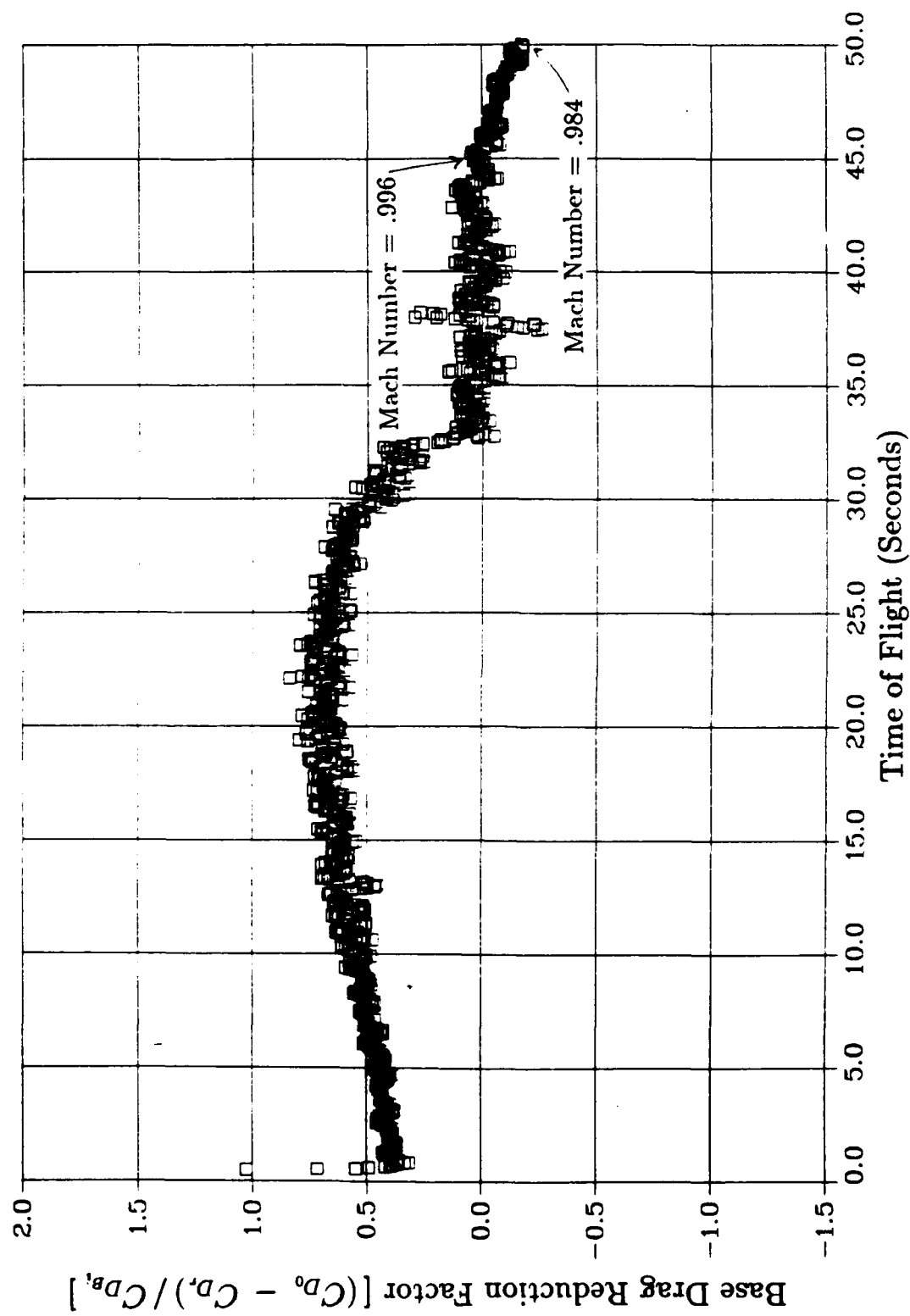


**Figure 12.** Base drag reduction factor versus time of flight for round number 4329 fired with propelling charge M203E2, 8R, at a quadrant elevation of 748 mils.

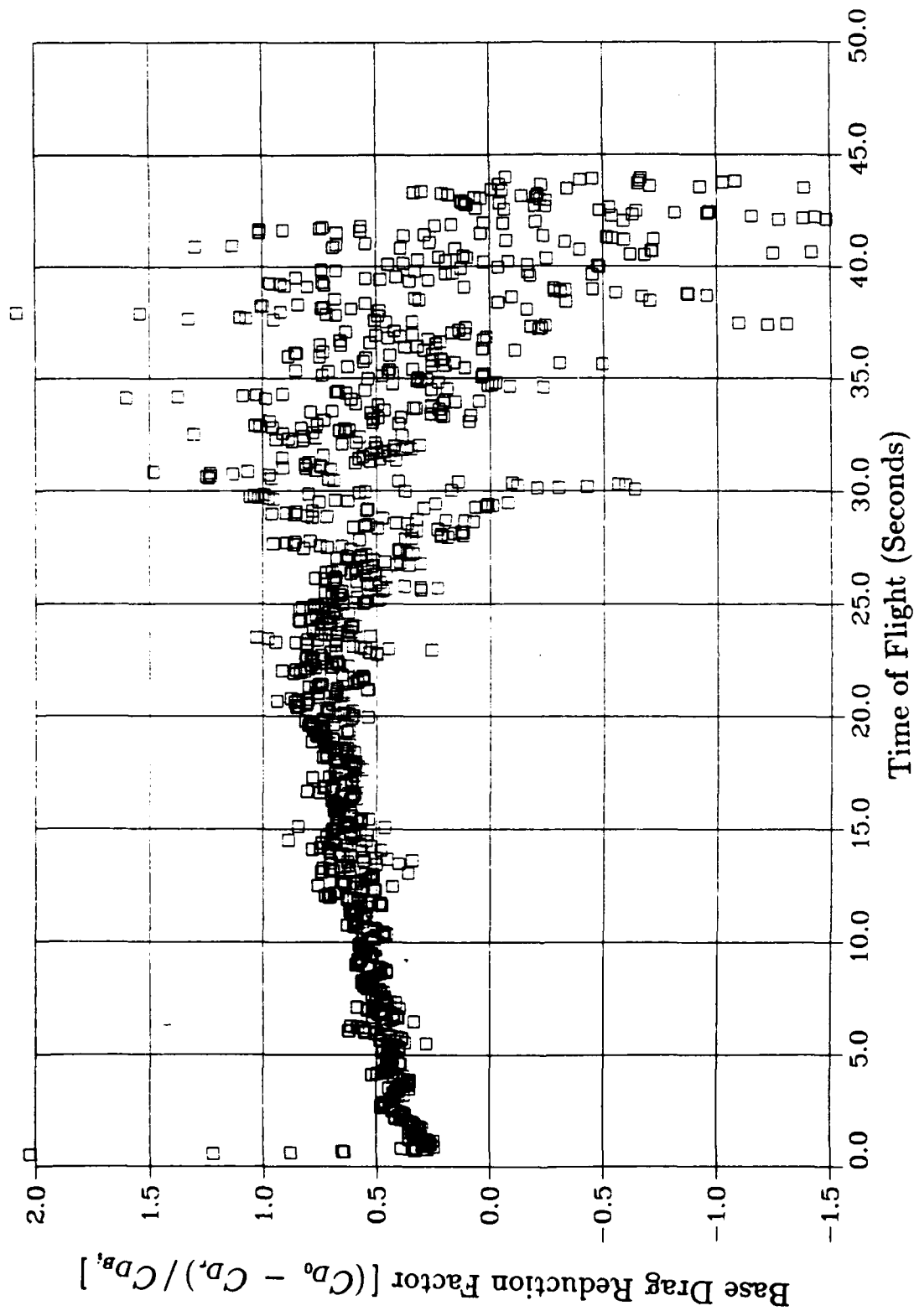


**Figure 13.** Base drag reduction factor versus time of flight for round number 4219 fired with propelling charge M203E2, 8R, at a quadrant elevation of 1147 mils.

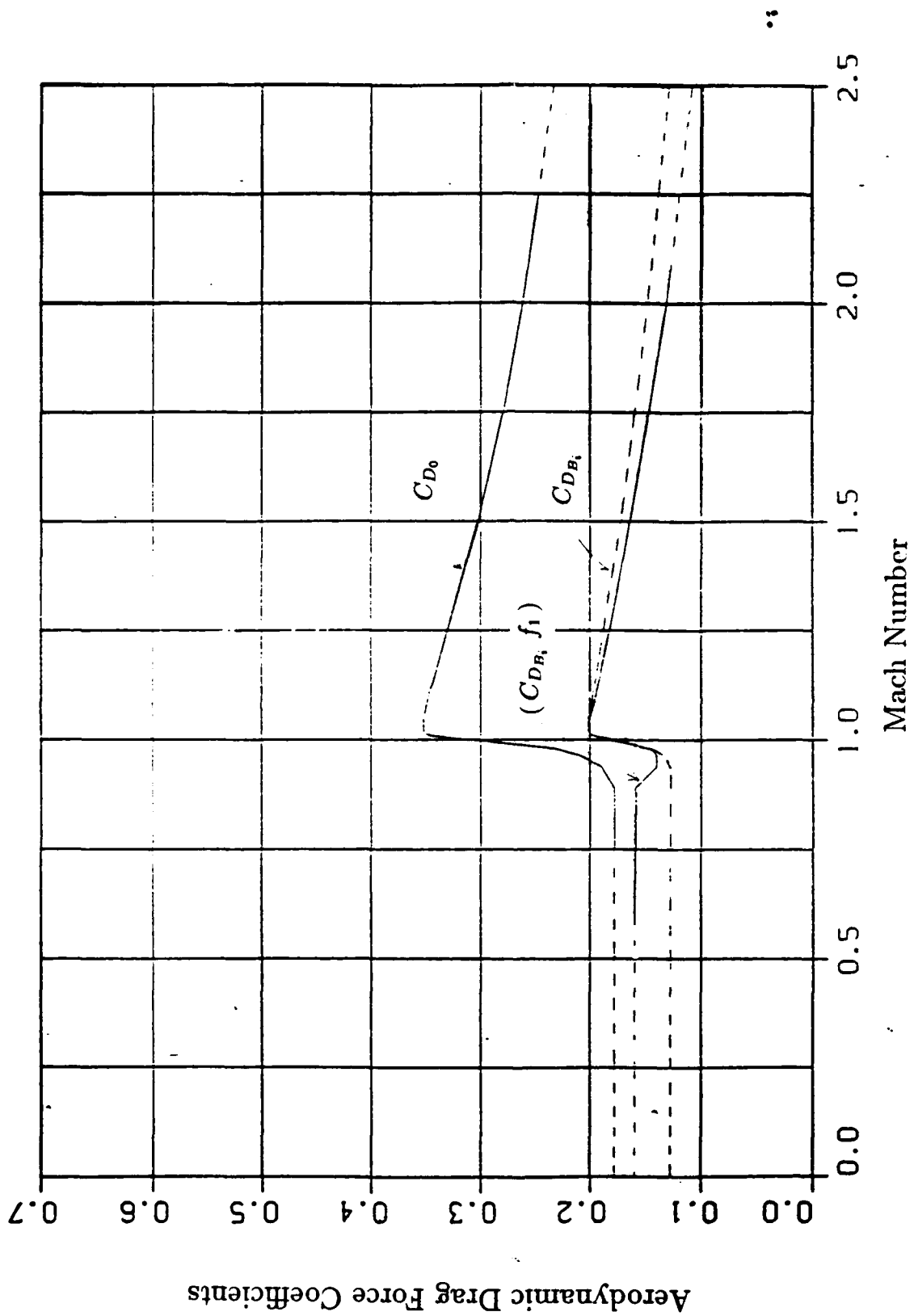


**Figure 14.** Aerodynamic drag force coefficients for the 155mm, DPICM, M864 base-burn projectile.

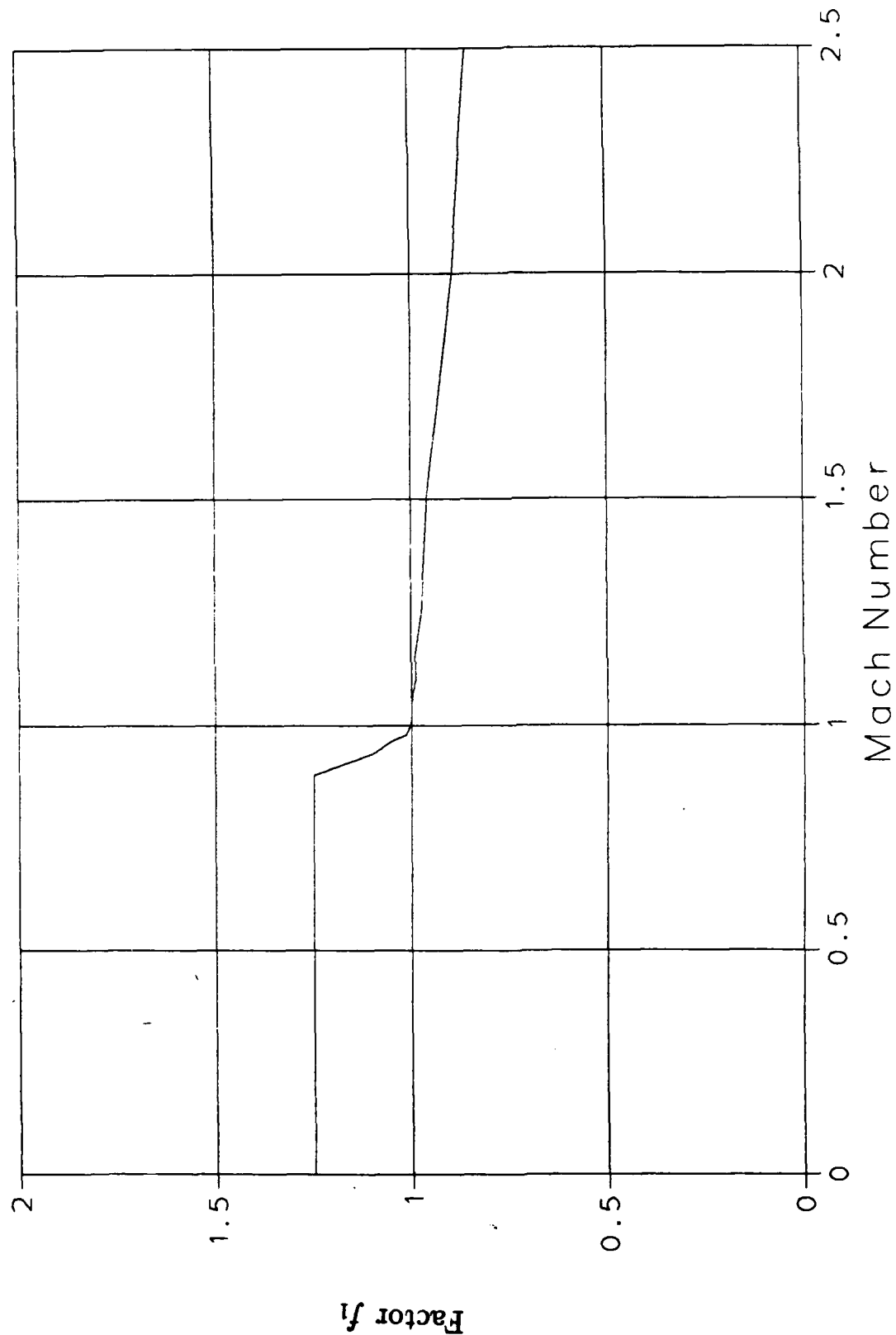


**Figure 16.** Factor  $f_1$  versus Mach number for the 155mm, DPICM, M864 projectile.

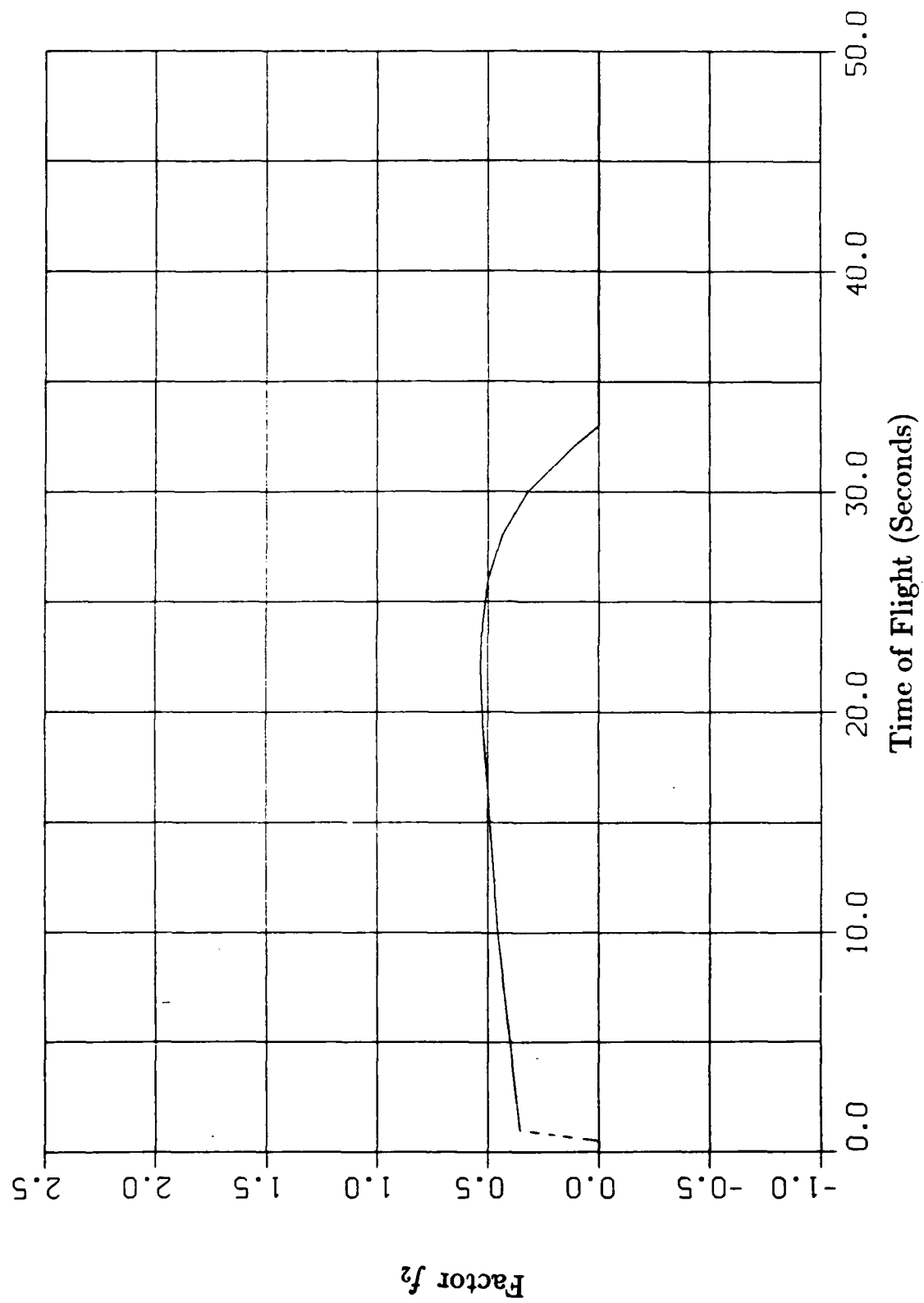


**Figure 16.** Factor  $f_2$  versus time of flight for the 155mm, DPICM, M864 projectile.

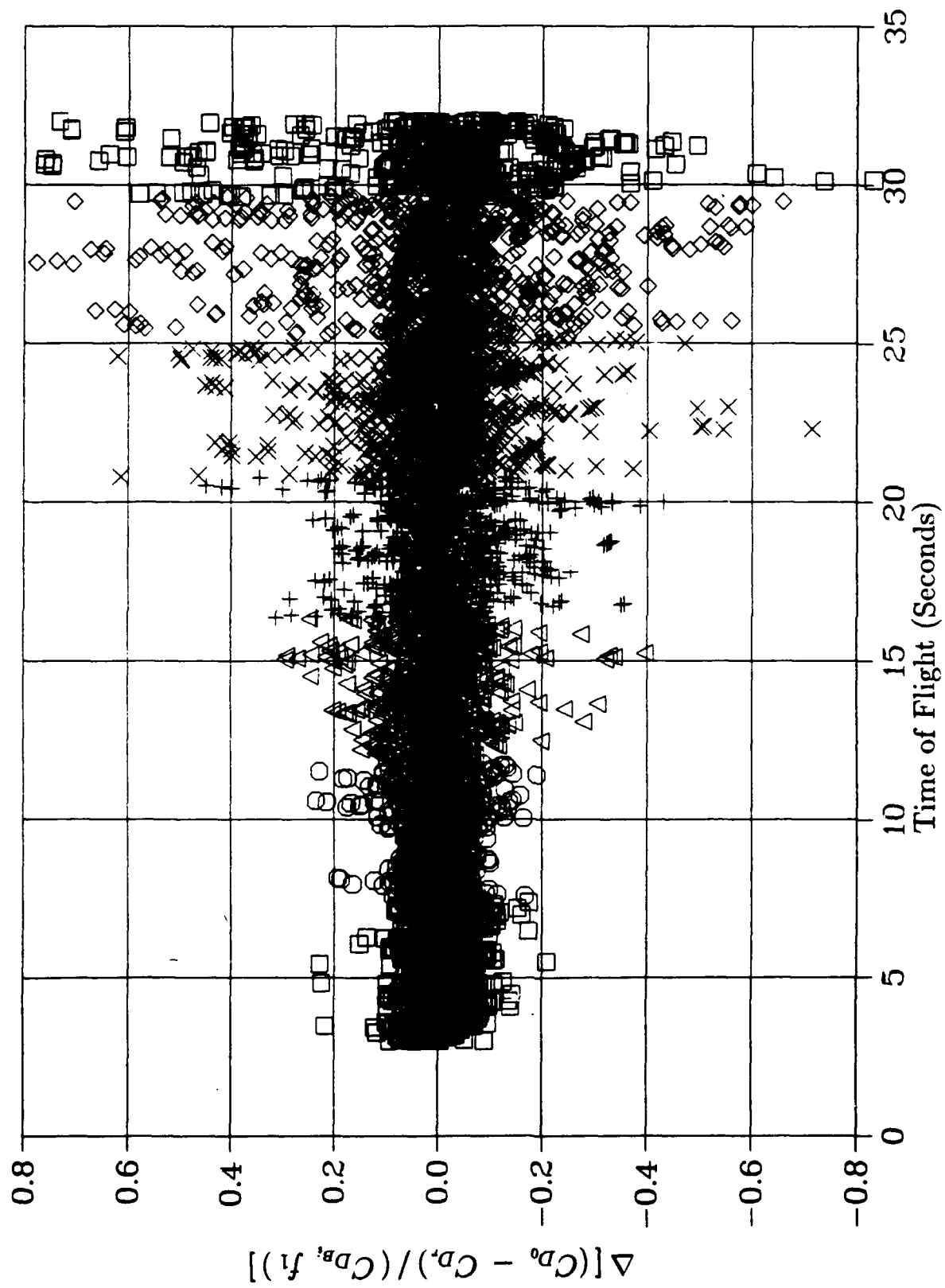


Figure 17. Residuals of the stepwise multiple regression analysis versus time of flight.

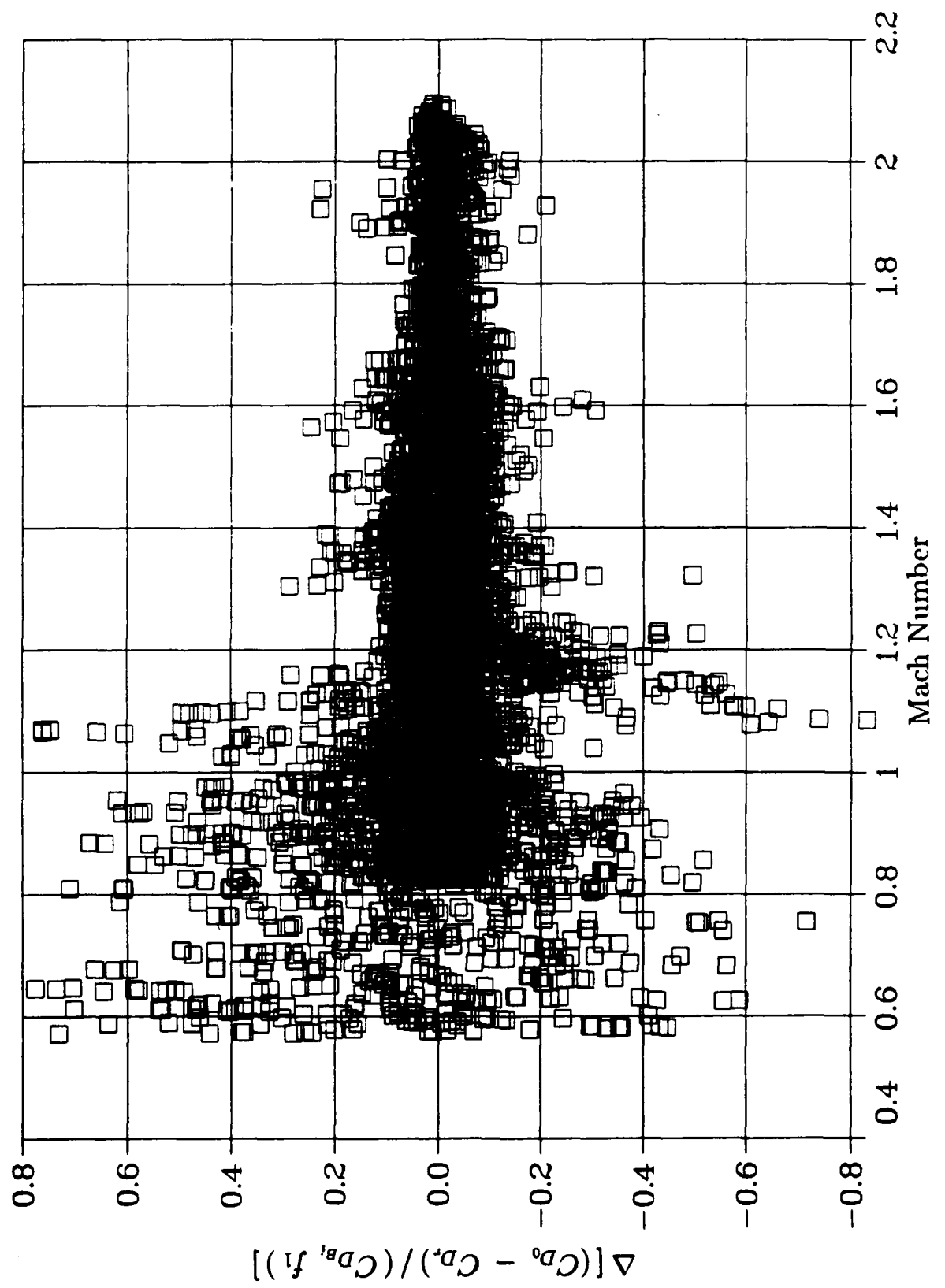


Figure 18. Residuals of the stepwise multiple regression analysis versus Mach number.

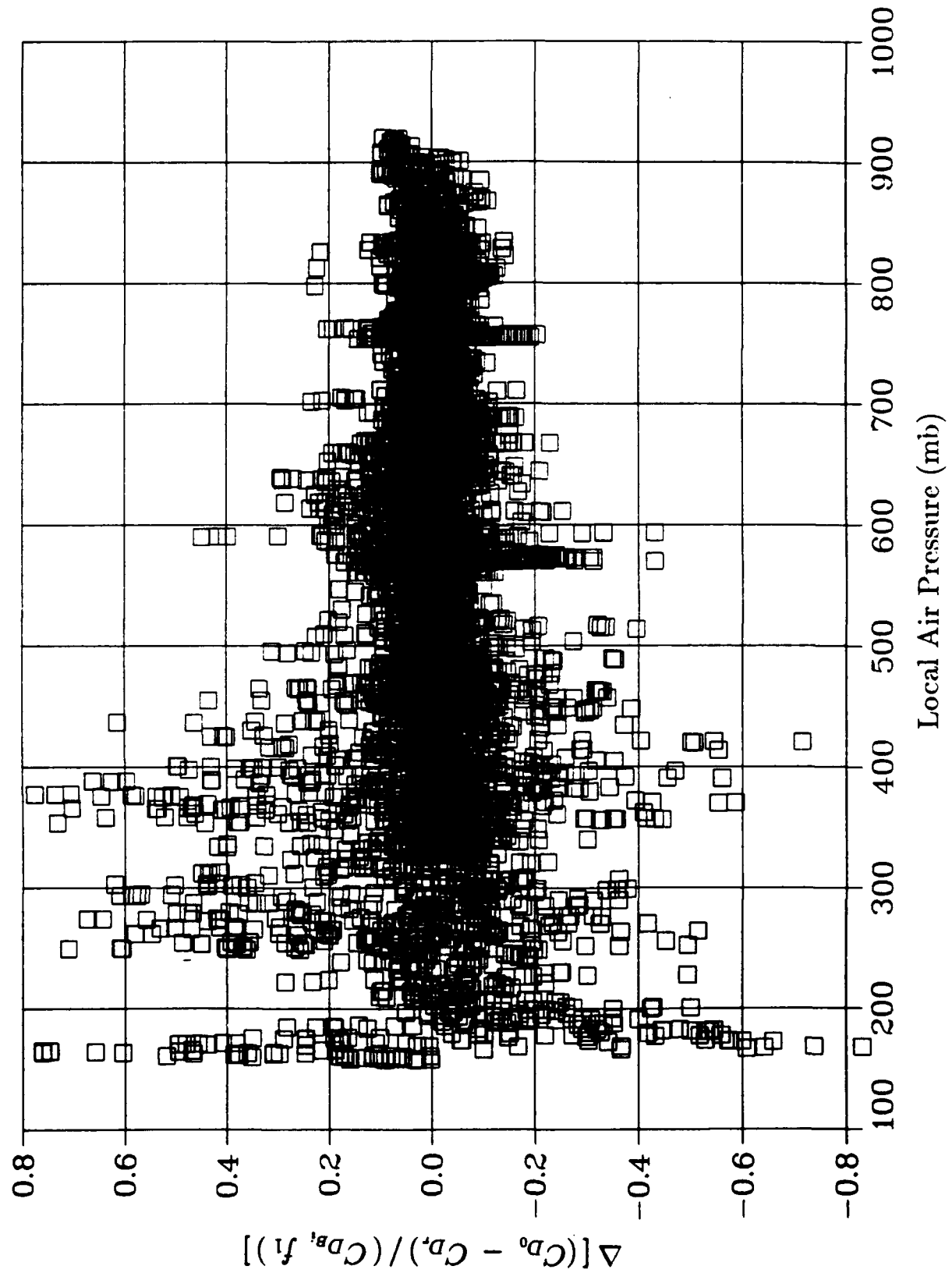


Figure 19. Residuals of the stepwise multiple regression analysis versus local air pressure.

## References

1. Lieske, R.F. and Reiter, M.L., "Equations of Motion for a Modified Point Mass Trajectory," US Army Ballistic Research Laboratory, Aberdeen Proving Ground, Maryland, BRL Report No. 1314, March 1966. (AD 485869)
2. NATO STANAG 4355 (Draft Edition 1), The Modified Point Mass Trajectory Model, February 1988.
3. Lieske, R.F. and Kochenderfer, J.W., "Determination of Performance Parameters for Fin-Stabilized Free-Flight Missiles," US Army Ballistic Research Laboratory, Aberdeen Proving Ground, Maryland, BRL Report No. 1349, December 1966. (AD 809790)
4. Lieske, R.F. and MacKenzie, A.M., "Determination of Aerodynamic Drag from Radar Data," US Army Ballistic Research Laboratory, Aberdeen Proving Ground, Maryland, BRL Memorandum Report No. 2210, August 1972. (AD 750564)
5. Nils-Erik Gunners, Kurt Andersson and Rune Hellgren, National Defense Research Institute (FOA) Tumba, Sweden, "Base-Bleed Systems for Gun Projectiles," Chapter 16, Volume 109, Dated 1988, Progress in Astronautics and Aeronautics, Gun Propulsion Technology. Published by the American Institute of Aeronautics and Astronautics, Inc., 370 L'Enfant Promenade, SW, Washington, DC 20024.
6. McCoy, R.L., "McDrag - A Computer Program for Estimating the Drag Coefficients of Projectiles," US Army Ballistic Research Laboratory, Aberdeen Proving Ground, Maryland, BRL Technical Report ARBRL-TR-02293, February 1981. (AD A098110)
7. Breaux, H.J., Campbell, L.W. and Torrey, J.C. "Stepwise Multiple Regression Statistical Theory and Computer Program Description," US Army Ballistic Research Laboratory, Aberdeen Proving Ground, Maryland, BRL Report No. 1330, July 1966. (AD 639955)



## List of Symbols

<u>Symbol</u>	<u>Definition</u>
$C_{D_0}$	zero yaw drag force coefficient
$C_{D_B}$	inert base-burn motor, base drag component of zero yaw drag force coefficient
$C_{D_r}$	radar determined drag force coefficient
$d$	reference diameter of projectile
$f_0$	factor as a function of quadrant elevation, previously identified as $i$ , used for matching experimental range firing data
$f_1$	factor used to represent the drag reduction as a function of Mach number
$f_2$	factor used to represent the drag reduction as a function of time of flight
$f_3$	factor used as a parameter for matching experimental range firing data
$f_4$	factor used to represent the drag reduction due to an apparent effect of local air pressure
$\vec{g}$	acceleration due to gravity
$m$	fuzed projectile mass at time $t$
$m_r$	reference fuzed projectile mass
$P$	air pressure at trajectory position
$P_r$	reference (standard) air pressure (1013.25 mb)
$C_{D_{\alpha}} (Q\alpha_e)^2$	yaw of repose drag term in the "Modified Point Mass Trajectory Model"
$r_t$	trajectory estimated, slant range magnitude
$\tilde{r}_t$	trajectory estimated, slant range
$\dot{r}$	HAWK radar determined, rate of change of slant range with time
$\ddot{r}$	time derivative of the HAWK radar determined, slant range rate of change
$\dot{r}_t$	trajectory estimated, rate of change of slant range with time
$\ddot{r}_t$	trajectory estimated, time derivative of the slant range rate of change

## List of Symbols (Continued)

<u>Symbol</u>	<u>Definition</u>
$\vec{u}_t$	trajectory estimated, velocity of the projectile with-respect-to the ground-fixed axes
$\dot{\vec{u}}_t$	trajectory estimated, acceleration of the projectile with-respect-to the ground-fixed axes
$\vec{u}_r$	velocity of the projectile with-respect-to the ground-fixed axis, determined from HAWK radar data and estimated trajectory
$\dot{\vec{u}}_r$	acceleration of the projectile with-respect-to the ground-fixed axes, determined from HAWK radar data and estimated trajectory
$v$	speed of projectile with-respect-to air
$\vec{v}$	velocity of the projectile with-respect-to air
$\vec{w}$	velocity of the air with-respect-to the ground (wind velocity)
$\vec{\Lambda}$	acceleration due to Coriolis effect
$\rho$	density (specific mass) of air

## Distribution List

<u>No. of Copies</u>	<u>Organization</u>	<u>No. of Copies</u>	<u>Organization</u>
12	Administrator Defense Technical Information Center ATTN: DTIC-DDA Cameron Station Alexandria, VA 22304-6145	1	Commander US Army Missile Command ATTN: AMSMI-RD-CS-R (DOC) Redstone Arsenal, AL 35898-5241
1	HQDA (SARD-TR) Washington, DC 20310-0001		
1	Commander US Army Materiel Command ATTN: AMCDRA-ST 5001 Eisenhower Avenue Alexandria, VA 22333-0001	2	Commander Armament RD&E Center US Army AMCCOM ATTN: SMCAR-MSI Picatinny Arsenal, NJ 07806-5000
1	Commander US Army Laboratory Command ATTN: AMSLC-DL Adelphi, MD 20783-1145	2	Commander Armament RD&E Center US Army AMCCOM ATTN: SMCAR-TDC Picatinny Arsenal, NJ 07806-5000
1	Commander US Army Armament, Munitions and Chemical Command ATTN: SMCAR-ESP-L Rock Island, IL 61299-5000	1	Director Benet Weapons Laboratory Armament RD&E Center US Army AMCCOM ATTN: SMCAR-LCB-TL Watervliet, NY 12189-4050
1	Commander US Army Tank Automotive Command ATTN: AMSTA-TSL Warren, MI 48397-5000	1	Director US Army TRADOC Analysis Command ATTN: ATAA-SL White Sands Missile Range, NM 88002-5502

## Distribution List (Continued)

<u>No. of Copies</u>	<u>Organization</u>	<u>No. of Copies</u>	<u>Organization</u>
1	Commandant US Army Infantry School ATTN: ATSH-CD-CSO-OR Fort Benning, GA 31905-5660	2	Commander US Army AMCCOM ATTN: SMCAR-CAWS-S Mr. R. DeKleine Mr. D. Griggs Picatinny Arsenal, NJ 07806-5000
1	Commander US Army Aviation Systems Command ATTN: AMSAV-DACL 4300 Goodfellow Blvd. St. Louis, MO 63120-1798	1	OPM Nuclear ATTN: AMCPM-NUC Picatinny Arsenal, NJ 07806-5000
1	Director US Army Aviation Research and Technology Activity Ames Research Center Moffett Field, CA 94035-1099	7	Commander Armament RD&E Center US Army AMCCOM ATTN: SMCAR-AET Mr. F. Scerbo Mr. J. Bera ATTN: SMCAR-AET-A Mr. R. Kline Mr. H. Hudgins
1	Air Force Armament Laboratory ATTN: AFATL/DLODL Eglin AFB, FL 32542-5000		ATTN: SMCAR-FSA Mr. F. Brody Mr. R. Kantenwein
1	AFWL/SUL Kirtland AFB, NM 87117-5800		ATTN: SMCAR-LCS-A Mr. J. Brooks Picatinny Arsenal, NJ 07806-5000
1	Director Requirements and Programs Directorate HQ, TRADOC Analysis Command ATTN: ATRC-RP Fort Monroe, VA 23651-5143	2	Commandant US Army Field Artillery School ATTN: ATSF-CCM ATTN: ATSF-GD Fort Sill, OK 73503
1	Commander TRADOC Analysis Command ATTN: ATRC Fort Leavenworth, KS 66027-5200	1	Director US Army Field Artillery Board ATTN: ATZR-BDW Fort Sill, OK 73503
1	Director TRADOC Analysis Command - White Sands Missile Range White Sands Missile Range, NM 88002-5502		

## Distribution List (Continued)

<u>No. of Copies</u>	<u>Organization</u>	<u>No. of Copies</u>	<u>Organization</u>
1	Commander US Army Dugway Proving Ground ATTN: STEDP-MT Mr. G. C. Travers Dugway, UT 84022	<b>Aberdeen Proving Ground</b>	
1	Commander US Army Yuma Proving Ground ATTN: STEYP-MTW Yuma, AZ 85365-9103	Director, USAMSAA ATTN: AMXSY-D AMXSY-MP Mr. H. Cohen AMXSY-RA Mr. R. Scungio AMXSY-GS Mr. B. King	
1	Headquarters US Marine Corps ATTN: Code LMW/30 Washington, DC 20380	Commander, USATECOM ATTN: AMSTE-TO-F AMSTE-TE-F Mr. W. Vomocil	
1	Director Sandia National Laboratories ATTN: Mr. A. Hodapp Division 1631 Albuquerque, NM 87185	Cdr, CRDEC, AMCCOM ATTN: SMCCR-MU SMCCR-RSP-A SMCCR -MSI	
1	Commander Naval Surface Weapons Center, Aerodynamics Branch, K-24, Building 402-12 ATTN: Dr. W. Yanta White Oak Laboratory Silver Spring, MD 20910	PM-SMOKE, Bldg. 324 ATTN: AMCPM-SMK-M Mr. J. Callahan	
1	Director Lawrence Livermore National Laboratory ATTN: Mail Code L-35 Mr. T. Morgan PO Box 808 Livermore, CA 94550	Director, USAHEL ATTN: SLCHE-FT	
		Commander, USACSTA ATTN: STECS-AS-H ATTN: STECS-EN-B	

USER EVALUATION SHEET/CHANGE OF ADDRESS

This laboratory undertakes a continuing effort to improve the quality of the reports it publishes. Your comments/answers below will aid us in our efforts.

1. Does this report satisfy a need? (Comment on purpose, related project, or other area of interest for which the report will be used.)

---

---

2. How, specifically, is the report being used? (Information source, design data, procedure, source of ideas, etc.)

---

---

3. Has the information in this report led to any quantitative savings as far as man-hours or dollars saved, operating costs avoided, or efficiencies achieved, etc? If so, please elaborate.

---

---

4. General Comments. What do you think should be changed to improve future reports? (Indicate changes to organization, technical content, format, etc.)

---

---

BRL Report Number \_\_\_\_\_ Division Symbol \_\_\_\_\_

Check here if desire to be removed from distribution list.

Check here for address change.

Current address: Organization \_\_\_\_\_  
Address \_\_\_\_\_  
\_\_\_\_\_

-----FOLD AND TAPE CLOSED-----

Director  
U.S. Army Ballistic Research Laboratory  
ATTN: SLCBR-DD-T(NEI)  
Aberdeen Proving Ground, MD 21005-5066

OFFICIAL BUSINESS  
PENALTY FOR PRIVATE USE \$300



NO POSTAGE  
NECESSARY  
IF MAILED  
IN THE  
UNITED STATES

---

---

---

---

---

---

---

---



Director  
U.S. Army Ballistic Research Laboratory  
ATTN: SLCBR-DD-T(NEI)  
Aberdeen Proving Ground, MD 21005-9989